RESEARCH ARTICLE

Proposing a Compartmental Model for Leprosy and Parameterizing Using Regional Incidence in Brazil

Rebecca Lee Smith*

Department of Pathobiology, University of Illinois College of Veterinary Medicine, Urbana, Illinois, United States of America

* rlsdvm@illinois.edu

Abstract

Hansen's disease (HD), or leprosy, is still considered a public health risk in much of Brazil. Understanding the dynamics of the infection at a regional level can aid in identification of targets to improve control. A compartmental continuous-time model for leprosy dynamics was designed based on understanding of the biology of the infection. The transmission coefficients for the model and the rate of detection were fit for each region using Approximate Bayesian Computation applied to paucibacillary and multibacillary incidence data over the period of 2000 to 2010, and model fit was validated on incidence data from 2011 to 2012. Regional variation was noted in detection rate, with cases in the Midwest estimated to be infectious for 10 years prior to detection compared to 5 years for most other regions. Posterior predictions for the model estimated that elimination of leprosy as a public health risk would require, on average, 44–45 years in the three regions with the highest prevalence. The model is easily adaptable to other settings, and can be studied to determine the efficacy of improved case finding on leprosy control.

Author Summary

Control of Hansen's disease, or leprosy, requires understanding how quickly the infection moves through the population and how long it takes to detect the disease. These rates vary regionally, resulting in differences in the number of people detected with disease each year. We have estimated the risk of infection and the rate of detection for this disease in each of the 5 regions of Brazil. This allowed us to predict the long-term impact of Brazil's current leprosy control program, which found that some regions of Brazil will require 44–45 years to eliminate leprosy as a public health risk, primarily due to the long delay in detection of cases.

Introduction

Hansen's disease (HD, or leprosy) is a chronic progressive disease caused in Brazil by infection with *Mycobacterium leprae*. Transmission is most likely through nasal droplets [1], and is

associated with socioeconomic status [2]. While leprosy is curable through chemotherapy [3], detection is often delayed [1], leading to more serious sequelae (including disfigurement and disability). The World Health Organization (WHO) has set a goal for elimination of leprosy as a public health problem, defined as a prevalence of <1/10,000 [4]. Several countries, including Brazil, have failed to meet that goal [5].

The Brazilian leprosy control program has been successful in decreasing the incidence of leprosy, but the prevalence remains high in 2 regions [5]. Movement towards elimination seems to have stagnated in these regions, possibly due to a downgrading of the importance of case finding [6]. Treatment of leprosy has been decentralized, so regional differences in case detection, and disease progression are to be expected [7]. Infection hotspots have also been noted in Brazil [8], leading to regional and sub-regional differences in transmission rates [5]. These may be related to socioeconomic factors, as a systematic review has found that socioeconomic inequalities associated with leprosy were large [9]. Prediction models must take these regional differences into account in order to accurately represent these differences and identify possible control points.

A number of models of leprosy have been proposed [10–21], and 6 of the base models from these studies were recently fitted to regional data from Brazil [22]. However, only one model takes into account much of the recent research on leprosy susceptibility [10,18], and it is an agent-based model that relies on specific population structures; the results of this model are quite useful on a regional level [23,24], but have not been applied to national-level results. The goal of this research is to produce a compartmental model that represents current understanding of leprosy susceptibility and pathogenesis, but that is also easily adaptable to different populations. Unknown parameters for this model will be fitted to regional incidence data from Brazil and analyzed to determine differences in control efficacy and their effect on the elimination target and long-term control.

Methods

All human data was anonymized at the source before usage [25]. As these data were publicly available and fully anonymized, no institutional review board approval was required.

A deterministic compartment model of leprosy (Fig 1) was designed to take into account current understanding of the disease. Briefly, individuals are divided into 3 categories: resistant (R, with probability $q_S = 1\text{-}p_s$), susceptible to paucibacillary infection (S_P, with probability $p_s{}^*p_p$), and susceptible to multibacillary infection (S_M, with probability $p_s{}^*q_p$ where $q_P = 1\text{-}p_p$). Resistance, q_s, is meant to convey both genetic resistance and socioeconomic protective factors [13,18]. Resistance to multibacillary infection, p_p, is meant to convey genetic resistance [18]; this value is higher than the observed proportion of new cases that are PB (0.8 vs. 0.54), but the discrepancy is explained by the high rate of self-cure among PB cases (α_{PN}). Resistant individuals (R) enter and leave the population without infection. Individuals with susceptibility to leprosy but genetic resistance to MB disease enter the paucibacillary (PB) track as susceptible (S_P). They may be exposed (E_P) at rate λ and eventually develop symptomatic PB disease (N_P) at rate γ_P. Paucibacillary disease either self-heals at rate α_{PN} or is detected and leads to treatment (T_P) at rate φ_P, either of which results in recovery (R_P) at rate α_{PT}. Recovered individuals may relapse to refractory disease (A_P) at rate σ_P, from which they can be detected and return to treatment at rate φ_P. Individuals with a genetic susceptibility to MB disease enter the population as susceptible (S_M) and may become exposed (E_M) at rate λ. Exposed individuals develop multibacillary disease (N_M) at rate γ_M and are diagnosed and entered into treatment (T_M) at rate φ_M. Treated individuals recover or leave treatment (R_M) at rate α_M and may relapse to refractory disease (A_M) at rate σ_M, from which they may be detected and return to treatment at
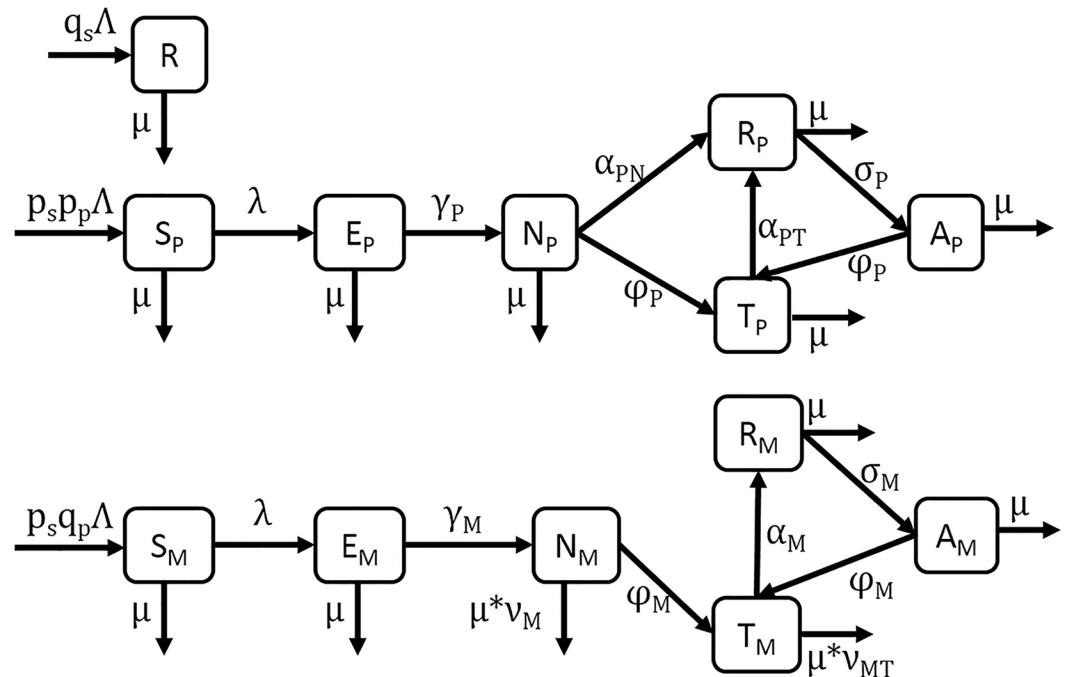
Fig 1. A compartment model of Hansen's disease.

rate φ_M. Multibacillary individuals are subject to a death rate that is proportionately higher than the general population, at ν_M for untreated individuals and ν_{MT} for treated individuals.

The force of infection, λ, is calculated as

$$\lambda = \frac{\beta_P(N_P + \theta_1 T_P + A_P) + \beta_M(N_M + \theta_2 T_M + A_M)}{N} \tag{1}$$

for the density-dependent model, where N is the total population size, β_P is the contribution of PB individuals to the force of infection, β_M is the contribution of MB individuals to the force of infection, θ_1 and θ_2 are the proportional decreases in infectiousness due to treatment of PB and MB individuals, respectively. Total population size (N) is calculated as the sum of all the compartments, and varies over time as births and deaths occur. For the sake of simplification, it is assumed that treated individuals are quickly rendered non-infectious [3] and therefore that $\theta_1 = \theta_2 = 0$. Thus, the force of infection becomes

$$\lambda = \frac{\beta_P(N_P + A_P) + \beta_M(N_M + A_M)}{N} \tag{2}$$

in the density-dependent model. Good estimates were available in the literature for most system parameters (see Table 1). However, estimates were unavailable for the transmission coefficients (β_P and β_M) and the true case detection rates (φ_P and φ_M), as these are likely to vary by locality and can be difficult to measure directly. These parameters were therefore estimated using the Sequential Monte Carlo approximate Bayesian Computation (SMC ABC) algorithm [26,27] applied to Brazilian incidence data, as described previously [22]. Briefly, the annual incidence of PB leprosy, $inc_{obs}^{PB}(y)$, and the annual incidence of MB leprosy, $inc_{obs}^{MB}(y)$, were obtained for each of the 5 regions of Brazil between 2000 and 2012 [28]. For each region, an initial parameter set (n = 100,000) was sampled from the prior distributions of the estimated parameters (a uniform distribution with a non-informative range, Table 1), and in subsequent

Table 1. Starting parameter values and ranges for a compartmental model of Hansen's Disease.
Regional values are set based on the demographics of the area providing observed data for fitting. Fitted values (unfitted assumption in parentheses) are estimated using Approximate Bayesian Computation.

Symbol	Description	Value
Λ	Rate at which individuals enter the population (year^{-1}) [28]	Regional
μ	Mortality rate (year^{-1}) [28]	Regional
β_P	Effective contact rate for PB (year^{-1}) [29]	Fitted (0.3, range 1e-5:5)
β_P^f	Effective contact rate for PB in a frequency-dependent model (year^{-1})	Fitted (7.5e-9, range 1.25e-13:6.25e-8)
β_M	Effective contact rate for MB (year^{-1}) [29]	Fitted (0.15, range 1e-5:5)
β_M^f	Effective contact rate for MB in a frequency-dependent model (year^{-1})	Fitted (3.75e-9, range 1.25e-13:6.25e-8)
φ_M	Case finding rate for MB (year^{-1}) [11]	Fitted (0.5, range 0.2–4)
φ_P	Case finding rate for PB (year^{-1}) [11]	Fitted (0.5, range 0.2–4)
p_s	Probability that an individual is susceptible to infection [11]	0.1
γ_M	Rate of progression to MB (year^{-1}) [11]	0.1
γ_P	Rate of progression to PB (year^{-1}) [11]	0.28
p_p	Probability that an individual is susceptible to PB infection only [11]	0.8
θ_1	Reduction factor of β for treated over untreated PB [30]	0
θ_2	Reduction factor of β for treated over untreated MB [30]	0
α_M	Recovery rate from treated MB (year^{-1}) [1]	1
α_{PN}	Self-recovery rate from PB (year^{-1}) [11]	0.224
α_{PT}	Recovery rate from treated PB (year^{-1}) [1]	2
σ_M	Rate of relapse to MB after recovery (year^{-1}) [11]	0.009
σ_P	Rate of relapse to PB after recovery (year^{-1}) [11]	0.001
v_M	Disease-induced proportional increase in mortality rate in untreated MB (year^{-1}) [31]	3.5
v_{MT}	Disease-induced proportional increase in mortality rate in treated MB (year^{-1}) (assumed)	1

PB = paucibacillary disease
MB = multibacillary disease

doi:10.1371/journal.pntd.0004925.t001

SMC particles (rounds), parameter sets were sampled from the immediately previous particle with a perturbation kernel. Each parameter set was used to simulate the incidence values between 2000 and 2010 (allowing 2011–2012 to be used for unconstrained validation), where incidence was assumed to be new individuals entering the treated category (T_P or T_M) from the untreated category (N_P or N_M). A distance function was calculated using the equation

$$d = \sum_{y=2000}^{2010} \left(inc_{obs}^{PB}(y) - inc_{pred}^{PB}(y) \right)^2 + \left(inc_{obs}^{MB}(y) - inc_{pred}^{MB}(y) \right)^2 \qquad (3)$$

where $inc_{pred}^{PB}(y)$ was assumed to be equal to $\varphi_P N_P(y)$, or the number of new PB cases entering treatment in year y, and $inc_{pred}^{MB}(y)$ was assumed to be equal to $\varphi_M N_M(y)$, or the number of new MB cases entering treatment in year y. It was assumed that recurrent infections (from A_P or A_M) were not included in the observed incidence. A parameter set was accepted if $d < \tau$, where τ was set equal to the 75th percentile of d in the previous particle. In each particle, the algorithm was repeated until 100,000 parameter sets were accepted; 10 particles were produced, with the 10th particle used to form the posterior distribution. The perturbation kernel was set to be a

uniform distribution with a range limited by ± the variance of each parameter in the previous particle.

Initial values in each of the compartments were determined analytically based on the parameters and observed prevalence. As the duration of treatment in MB disease is twice the duration of treatment in PB disease under MDT, the observed prevalence was assumed to be divided between $T_M(0)$ and $T_P(0)$ with the ratio $2 * \frac{incidence(MB)}{incidence(PB)}$. The ratio of $N_i(0){:}T_i(0)$, $E_i(0){:}N_i(0)$, $R_i(0){:}T_i(0)$, and $A_M(0){:}N_M(0)$, where $i \in \{M,P\}$, were set empirically in a multi-step process similar to that described previously [22]. Briefly, the ratios were adjusted manually for each region such that the model, simulated with the assumed values in Table 1, predicted the incidence of both PB and MB cases in that region with less than 10% deviation from the observed values in 2000 (the first year of observation) and 2002 (the year of peak incidence in most regions). The model was then fitted with the initial population distribution determined by these ratios, and the median of the estimated distribution for each fitted parameter was used to predict incidence of both PB and MB cases in each region. If the predicted incidences in 2000 or 2002 deviated from observed values in any region by more than 10%, the ratios were again adjusted manually to correct the deviation and the model was re-fitted. This process repeated until the median of the estimated distribution for each fitted parameter was able to predict incidence of PB and MB cases in each region with less than 10% deviation from observed values in both 2000 and 2002.

As density-dependent transmission was assumed, but is known to be a simplification of true human contact rates [32], the above process was repeated for a frequency-dependent transmission model. In this model, the force of infection λ_f becomes

$$\lambda_f = \beta_P^f(N_P + A_P) + \beta_M^f(N_M + A_M) \tag{4}$$

where β_P^f and β_M^f are adjusted from the density-dependent model to account for population size. The results of the frequency and density dependent models were compared using Bayes factor analysis, in which the Bayes factor was the ratio of the summed distance in all regions, corrected for differences in regional population size, across a weighted sample of 1,000 posterior parameter sets.

The results of the best-fitting regional model (frequency or density dependent) were examined for similarity between distributions, and 3 hierarchical fittings were considered: transmission parameters (β_M, β_P) shared across regions (V1), transition parameters (φ_M, φ_P) shared across regions (V2), all parameters (β_M, β_P, φ_M, φ_P) shared across regions (V3), and sharing no parameters (the regional model described above, V4). In the hierarchical models, the distance function was altered to

$$d = \sum_r \sum_{y=2000}^{2010} \left(inc_{obs}^{PB}(y,r) - inc_{pred}^{PB}(y,r) \right)^2 + \left(inc_{obs}^{MB}(y,r) - inc_{pred}^{MB}(y,r) \right)^2 \Big/ N_r \tag{5}$$

where r represents the region and N_r is the population of region r in 2000. Hierarchical models were compared to each other and the regional model using Bayes factor analysis, in which the Bayes factor was the ratio of the summed distance in all regions, corrected for differences in regional population size, across a sample of 1,000 posterior parameter sets weighted by the inverse of their summed regional distances (Eq 5).

In order to check the consistency of the model results, data were simulated for each region using the median of the best fitted value from the preferred hierarchical model. These data were then used to repeat the full model selection and parameterization process, including

hierarchical model selection and parameterization. Results were compared to the simulated input values.

Posterior predictions were produced using a weighted sample of 1,000 parameter sets from the posterior distribution of both the preferred hierarchical model and the regional model, and outcomes of interest were predicted from this sample. Outcomes were the time to elimination in years (t_{elim}) and the predicted incidence overall and of MB and PB cases in the year 2050 (i_{2050}, iM_{2050}, and iP_{2050}, respectively).

All models and fitting were performed in R 3.0.3,[33] which was accessed through the Revolution R Analytics interface (copyright 2014 Revolution Analytics, Inc.).

Results

The median and range of each parameter for the each of the model fits are shown in Table 2. Transmission and transition parameters were similar between the density-dependent and frequency-dependent models. Bayes factor analysis identified the frequency-dependent model as having the lowest summed deviance from the observed incidence. As a result, the frequency-dependent model was used for hierarchical model fitting.

Bayes factor analysis identified the regional version as having the lowest summed deviance from the observed incidence, although the preference for the regional version was not strong (Bayes Factor of 1.2 to 2.1, compared to the hierarchical models). Transmission coefficients were estimated to be similar in all regions even in the regional model, but transition rates had high variability between regions. Transition rates were lower in the Midwest for all individuals, higher in the South and Southeast for MB individuals, and higher in the North for PB individuals.

The final distribution of the initial population, as determined by the empirical process, is shown in Fig 2 for each region and model fit. The number of latent and undetected individuals was the most variable across models, with the density-dependent model requiring higher numbers of latent individuals to reproduce the initial and peak incidence in each region.

Posterior predictions for the preferred hierarchical model and the regional model are shown in Fig 3 and Table 3. The results show that the fit underestimated PB incidence in the North and Midwest and MB incidence in most regions in later years. The South and Southeast reported incidences below the elimination threshold in 2001, and this was also predicted to be possible by the model, although the average time to elimination was predicted to be 2002 and 2007, respectively. On average, the North and Midwest were predicted to reach the elimination threshold by 2045, while the Northeast was predicted to reach the elimination threshold by 2044. However, the ranges of values were wide, indicating that the Northeast could require up to the year 2053 to reach the elimination threshold.

Simulation results (Table 4) show that the model was able to predict the simulated values in most cases. The exceptions were the values of φ_M and φ_P, which tended to overestimate the true value, and the values of β_M and β_P in the density-dependent model, which tended to underestimate the true value.

Discussion

This study presents a compartmental model for Hansen's Disease that takes into account the current understanding of the disease but that is computationally simple and easy to adapt. The structure of this model differs from that of Meima et al. [11] in 2 ways. First, this model assumes that the 90% of people who never develop leprosy are inherently resistant, rather than self-healing. Second, this model assumes that the 80% of susceptibles who will only develop PB disease are again inherently resistant to MB disease. That allows us to separate the relapsed

Table 2. Posterior distribution median and 95% prediction intervals determined by ABC fitting of Approximate Bayesian Computation models for Hansen's Disease to data from the 5 regions of Brazil. Version 4 consisted of fitting the regional best-fit model to each region's observed data separately with both frequency and density-dependent transmission assumptions; all other versions used a hierarchical structure with density-dependent transmission in which at least some parameters were shared across regions, and fitting was done simultaneously across all 5 regions. Mean error refers to the average value of d per iteration of each version, based on a sample of 1,000 iterations, with confidence intervals based on 100 samples of 100 iterations each.

V[a]	Reg.[c]	β_M	β_P	φ_M	φ_P	Mean Error
1	N			0.41 (0.1–2.6)	0.45 (0.11–2.9)	
	NE			0.01 (0.01–0.01)	0.01 (0.01–0.012)	2.1e-14
	SE	1.4 (0.011–2.5)	0.75 (0.0012–2.4)	0.01 (0.01–2.7)	0.01 (0.01–2.7)	2e-14-
	S			0.01 (0.01–2.7)	0.01 (0.01–2.6)	-2.3e-14)
	MW			0.47 (0.11–3)	0.41 (0.057–2.7)	
2	N	1.5 (0.0031–2.5)	1.5 (0.004–2.5)			
	NE	0.84 (0.0031–2.4)	1.3 (0.0013–2.5)			1.3e-14
	SE	1.1 (0.0024–2.5)	1.2 (0.0015–2.5)	0.19 (0.15–0.25)	0.23 (0.17–0.32)	(1.2e-14-
	S	1.1 (0.004–2.5)	1.2 (0.0073–2.5)			1.3e-14)
	MW	1.5 (0.0057–2.5)	1.3 (0.0085–2.5)			
3	All	1.6 (0.0036–2.5)	1 (0.0036–2.5)	0.19 (0.14–0.28)	0.23 (0.16–0.35)	1.7e-14 (1.7e-14-1.8e-14)
4$_f$[b]	N	2.2 (1.4–2.5)	1.4 (0.0027–2.4)	0.2 (0.2–0.22)	0.52 (0.39–0.73)	
	NE	2.1 (1.5–2.5)	1.1 (0.59–1.6)	0.2 (0.2–0.21)	0.2 (0.2–0.2)	1.0e-14
	SE	1.5 (0.68–2.5)	0.66 (0.007–1.1)	0.51 (0.44–0.63)	0.2 (0.2–0.21)	(1.0e-14-
	S	1.8 (0.76–2.5)	0.86 (0.0024–1.7)	0.46 (0.43–0.52)	0.2 (0.2–0.2)	1.0e-14)
	MW	1.7 (1.2–2.5)	0.26 (9.1e-3-0.56)	0.01 (0.01–0.01)	0.01 (0.01–0.01)	
4$_d$	N	0.7 (0.5–0.8)	0.7 (8.9e-4-0.8)	0.2 (0.2–0.22)	0.52 (0.39–0.73)	
	NE	2.5 (1.8–3.0)	1.4 (0.7–1.9)	0.2 (0.2–0.21)	0.2 (0.2–0.2)	1.4e-14
	SE	2.7 (1.2–4.6)	1.2 (1.3e-2-2.1)	0.51 (0.44–0.63)	0.2 (0.2–0.21)	(1.4e-14-
	S	1.1 (0.5–1.6)	0.5 (1.6e-3-1.1)	0.46 (0.43–0.52)	0.2 (0.2–0.2)	1.4e-14)
	MW	0.1 (8.2e-3-0.2)	0.01 (4.8e-5-0.1)	0.01 (0.01–0.01)	0.01 (0.01–0.01)	

[a]Version of the hierarchical structure sharing parameters across 5 regions of Brazil: 1) all parameters shared; 2) transmission parameters shared; 3) transition parameters shared; 4$_f$) no parameters shared, frequency-dependent transmission; 4$_d$) no parameters shared, density-dependent transmission

[b]Density-dependent transmission parameters have been transformed to be comparable to frequency-dependent transmission parameters by multiplying the estimated values by the population size in the year 2000.

[c]Region: N = North (Acre, Amapá, Amazonas, Pará, Rondônia, Roraima, and Tocantins States), NE = Northeast (Alagoas, Bahia, Ceará, Maranhão, Paraíba, Pernambuco, Piauí, Rio Grande do Norte, and Sergipe states), SE = Southeast (Espírito Santo, Minas Gerais, Rio de Janeiro, and São Paulo states), S = South (Paraná, Rio Grande do Sul, and Santa Catarina states), MW = Midwest (Goiás, Mato Grosso, Mato Grosso do Sul, and Distrito Federal states)

doi:10.1371/journal.pntd.0004925.t002

cases appropriately, such that only those recovered from MB disease relapse to MB disease. These assumptions also allow for including differences of susceptibility in a compartmental model, which is less computationally intensive, easier to fit to data, and easy to adapt to other populations or across larger and more diverse regions. However, Ridley-Jopling classification allows for borderline cases which can cross between PB and MB groups during relapse.[34] While it would be advantageous to capture the full diversity of leprosy presentation in future models, the parameterization of such models will require improved reporting; at present, Brazil reports only the PB and MB classifications of detected cases.[25]

Many studies at the national or regional level will report a "case detection rate". This, however, is not the true case finding rate represented by φ_M and φ_P in this model. It is, instead, the annual observed incidence, and uses the population as the denominator, not the delay in diagnosis. This is an important difference: a high "case detection rate" could indicate an outbreak rather than fast detection, while the true case finding rate only represents the time necessary to
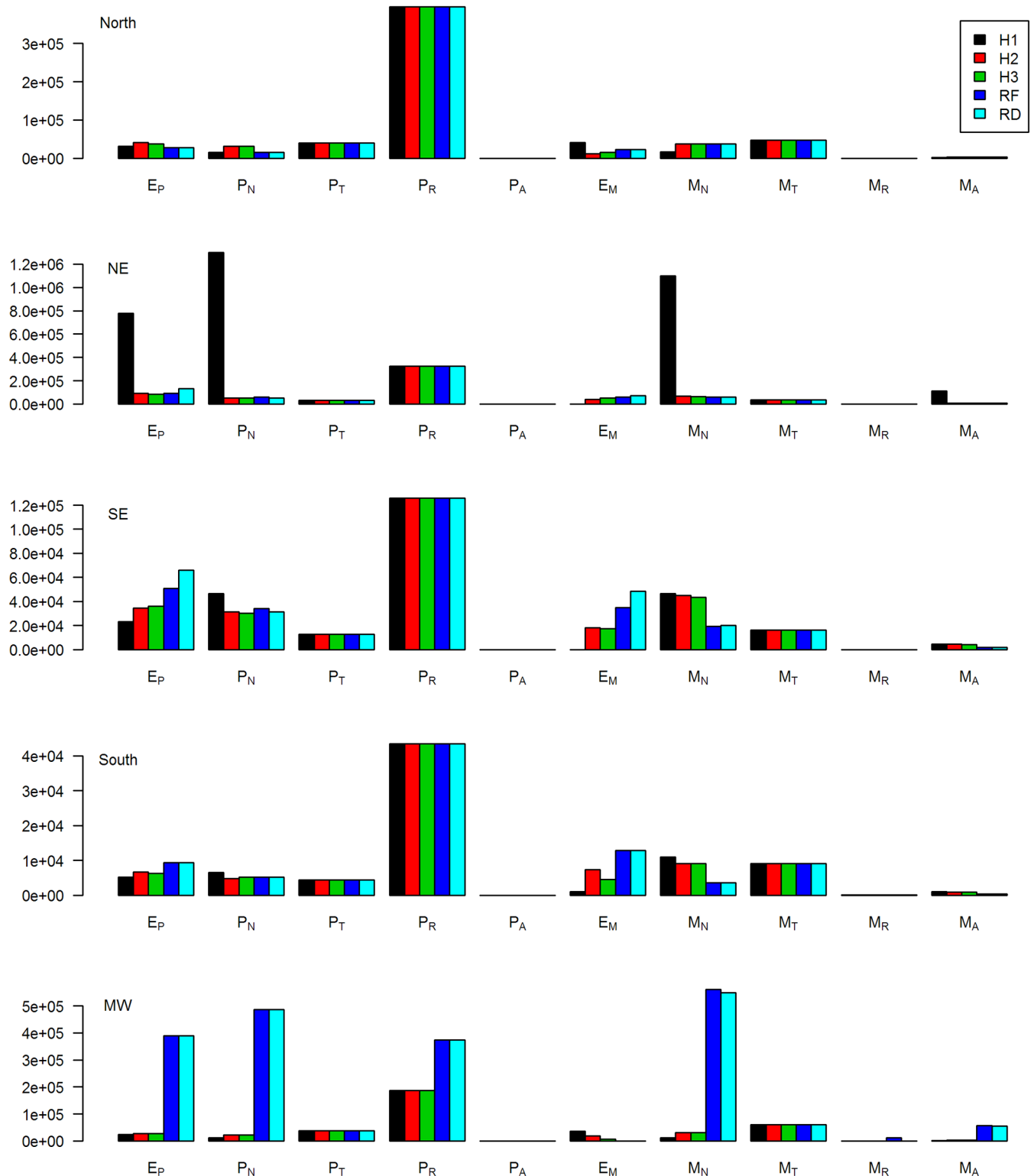
Fig 2. Number of initial population in infected categories for a dynamic model of *Mycobacterium leprae* in Brazilian regions. The colors represent different model fits (black H1: fitted transmission parameters shared across all regions, red H2: fitted transition parameters shared across all regions, green H3: all fitted parameters shared across all regions, dark blue RF: no fitted parameters shared across regions, and light blue RD: no fitted parameters shared across regions and density-dependent transmission). Each row is a different region. The infected categories are: E_P, latent paucibacillary (PB); P_N, undetected PB; P_T, treated PB; P_R, recovered PB; P_A, recurrent PB; E_M, latent multibacillary (MB); M_N, undetected MB; M_T, treated MB; M_R, recovered MB; and M_A, recurrent MB.

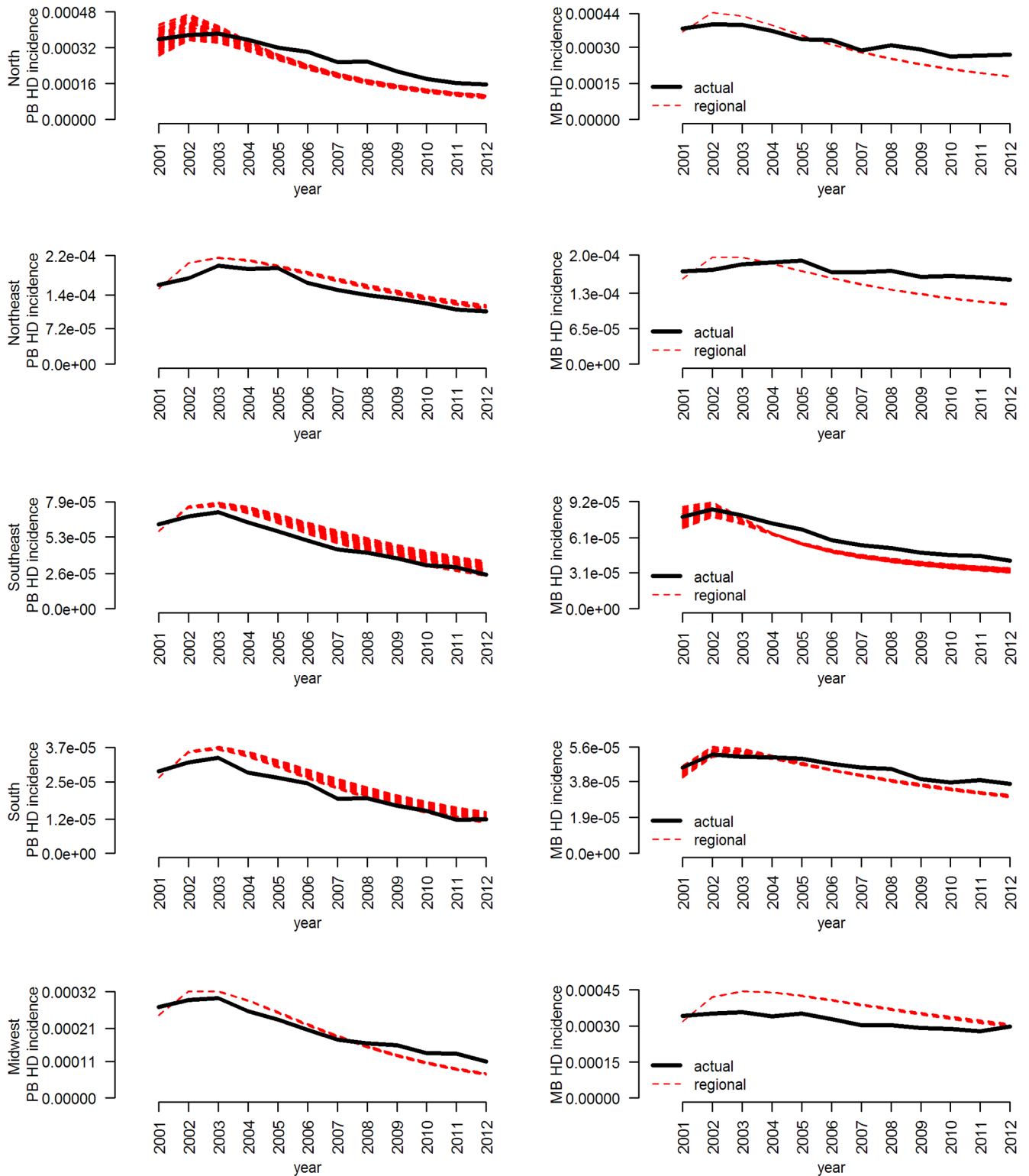doi:10.1371/journal.pntd.0004925.g002

Fig 3. Posterior predictions for incidence and multibacillary (MB) incidence of the compartmental model of Hansen's disease for the regions of Brazil, compared to the observed values for 2000–2012. Unknown parameters were fitted to each region individually. All models were fit using Approximate Bayesian Computation with the Sequential Monte Carlo algorithm.

doi:10.1371/journal.pntd.0004925.g003

Table 3. Posterior predictions (mean and range) from the regional model for Hansen's Disease fit to regional data from Brazil. Incidence of Hansen's Disease in the year 2050 is reported overall (i_{2050}) and for multibacillary (iM_{2050}) and paucibacillary (iP_{2050}). The time to elimination (t_{elim}) was calculated as the year in which overall incidence was $\leq 1/10,000$, starting from 2001.

Region	i_{2050} (/10,000)	iM_{2050} (/10,000)	iP_{2050} (/10,000)	t_{elim}
North	0.91 (0.83–0.98)	0.57 (0.55–0.59)	0.34 (0.29–0.4)	45 (40–49)
Northeast	0.99 (0.92–1.1)	0.54 (0.52–0.56)	0.45 (0.41–0.5)	44 (38–53)
Southeast	0.22 (0.17–0.28)	0.14 (0.12–0.17)	0.071 (0.042–0.11)	7.3 (7–8)
South	0.16 (0.15–0.17)	0.13 (0.12–0.13)	0.031 (0.024–0.039)	1 (1–1)
Midwest	0.89 (0.88–0.89)	0.66 (0.63–0.69)	0.22 (0.2–0.25)	45 (44–46)

doi:10.1371/journal.pntd.0004925.t003

identify a clinical case. We found that the range of potential case finding rates was fairly similar across most regions, but that cases were estimated to be infectious for 5 years in most cases before treatment was initiated. This agrees with the findings of multiple studies [35,36], where people delayed seeking treatment partly from an assumption that the symptoms were not serious and potentially from a worry of the stigma attached to a diagnosis [37]. It also falls into the range assumed by previous models within Brazil for this time period [24]. In a modeling study,

Table 4. Posterior distribution median and 95% prediction intervals determined by ABC fitting of Approximate Bayesian Computation models for Hansen's Disease to data simulated by the best-fit model. The values fit were $\beta_M = 1.9$, $\beta_P = 1.2$, $\varphi_M = 0.2$, and $\varphi_P = 0.2$ for all but the North, where $\varphi_2 = 0.46$. Version 4 consisted of fitting the regional best-fit model to each region's observed data separately with both frequency and density-dependent transmission assumptions; all other versions used a hierarchical structure with density-dependent transmission in which at least some parameters were shared across regions, and fitting was done simultaneously across all 5 regions. Values in bold italics contained the simulated value within their range. Mean error refers to the average value of d per iteration of each version, based on a sample of 1,000 iterations, with confidence intervals based on 100 samples of 100 iterations each.

V[a]	Region	β_M	β_P	φ_M	φ_P	Mean Error
1	North			*0.44 (0.23–1.2)*	*0.42 (0.2–1.2)*	
	Northeast			*0.2 (0.2–2.1)*	*0.2 (0.2–0.86)*	5.7e-15
	Southeast	*1.2*	*0.89*	*0.2 (0.2–2.8)*	*0.2 (0.2–2.7)*	(5.4e-15-
	South	*(0.00049–2.5)*	*(0.00049–2.4)*	*0.2 (0.2–2.6)*	*0.2 (0.2–2.6)*	6.1e-15)
	Midwest			0.45 (0.22–1.3)	*0.2 (0.2–0.33)*	
2	North	*1.6 (0.00073–2.5)*	*1.3 (0.005–2.5)*			
	Northeast	*1.1 (0.00073–2.5)*	*1.6 (0.00022–2.5)*			3.7e-15
	Southeast	*1.3 (0.0038–2.5)*	*1.2 (0.0031–2.5)*	0.5 (0.39–0.69)	0.47 (0.35–0.65)	(3.5e-15-
	South	*1.3 (0.0054–2.5)*	*1.2 (0.00095–2.5)*			3.8e-15)
	Midwest	*1.5 (2.8e-05-2.5)*	*1.5 (0.00043–2.5)*			
3	All	*2.1 (0.24–2.5)*	*1.6 (3e-04–2.5)*	0.49 (0.39–0.7)	0.46 (0.34–0.66)	3.6e-15 (3.3e-15-3.7e-15)
4_f[b]	North	*2 (0.0086–2.5)*	*1.2 (0.00018–2.5)*	0.5 (0.4–0.67)	0.49 (0.39–0.64)	
	Northeast	*2.4 (1.8–2.5)*	2.1 (1.3–2.4)	0.48 (0.4–0.64)	0.44 (0.36–0.56)	3e-15
	Southeast	*2.4 (1.8–2.5)*	2.2 (1.4–2.5)	0.49 (0.36–0.83)	0.27 (0.2–0.38)	(2.8e-15-
	South	*2.1 (0.2–2.5)*	*1.3 (0.00069–2.5)*	0.49 (0.31–0.97)	0.46 (0.22–1.2)	3.1e-15)
	Midwest	*2 (0.00078–2.5)*	*1.2 (0.00024–2.4)*	0.5 (0.4–0.7)	0.49 (0.37–0.69)	
4_d	North	*1.4 (0.13–3)*	*0.85 (1e-5-2.3)*	0.48 (0.39–0.62)	*0.44 (0.37–0.63)*	
	Northeast	1e-5 (1e-5-1.5)	1e-5 (1e-5-0.6)	*0.2 (0.2–0.2)*	*0.2 (0.2–0.2)*	1.7e-14
	Southeast	*2.8 (2–4.7)*	*1.3 (1e-5-2.4)*	*0.2 (0.2–0.2)*	*0.2 (0.2–0.2)*	(1.6e-14-
	South	0.36 (1e-5-1.5)	1e-5 (1e-5-0.97)	*0.2 (0.2–0.2)*	*0.2 (0.2–0.21)*	1.7e-14)
	Midwest	1e-5 (1e-5-1e-5)	1e-5 (1e-5-1e-5)	*0.2 (0.2–0.2)*	*0.2 (0.2–0.2)*	

[a]Version of the hierarchical structure sharing parameters across 5 regions of Brazil: 1) all parameters shared; 2) transmission parameters shared; 3) transition parameters shared; 4_f) no parameters shared, frequency-dependent transmission; 4_d) no parameters shared, density-dependent transmission
[b]Frequency-dependent transmission parameters have been transformed to be comparable to density-dependent transmission parameters.

doi:10.1371/journal.pntd.0004925.t004

Fischer et al. [10] found that contact tracing was important to avoid the diagnostic delay; contact tracing was decreased in India in order to meet WHO case detection rate goals, and the result was treatment delays [38], which would produce a long-term effect of higher incidence and, eventually, higher case detection rates. Importantly, our model predicted that cases in the Midwest were infectious for an average of 100 years before detection, an unrealistic value indicating that the true detection rate of cases is too low to estimate properly. If true, this could indicate a public health failing that should be addressed. This difference in detection rate between regions could be socio-economic in origin, as the three regions predicted to have low detection rates (Northeast, North, and Midwest) also have lower GDP per capita. Similar regional health disparities have been noted for ischaemic heart disease [39] and laryngeal cancer [40] mortality, suggesting regional disparities in health care [41].

The decision was made to compare density- and frequency-dependent models, despite the fact that leprosy is considered to be a disease of close contact and therefore would be classically considered to have density-dependent transmission. This is due to the limitations of a model such as this, caused by the homogeneous mixing assumption, in capturing the limited number of close contacts any individual is likely to have. Thus, while a disease may be truthfully density-dependent, it may behave mathematically as a frequency-dependent disease. The results of this study show that the density-dependent model was slightly preferred to the frequency-dependent model. This question would not arise with an individual-based model, such as SIM-COLEP [42], but those models are not as easy to adapt as they must rely on population-specific characteristics in their design, which may require parameters that are not locally available. The goal of this study was to provide an adaptable model that was still able to capture the regional dynamics of leprosy spread. The preference of the regional model supported this decision, but the preference was not strong, indicating that some national-level models may be as informative as the regional models.

Several models assume that PB individuals are non-infectious [11]. We observed that PB individuals did contribute to the force of infection, although with roughly half to two-thirds the strength of MB individuals. In other mycobacterial diseases, less infectious individuals have been found to be potentially important in maintaining the endemicity of the infection [43,44]. This highlights the importance of diagnosing and treating all cases; although the PB cases do not have as serious sequelae as the MB cases, they may serve to maintain the infection in a region. With regards to the intra-regional variation in transmission parameters, we found that higher transmission parameters were predicted in regions with higher incidence. This is to be expected, and highlights the ability of the model fitting to identify regional differences.

The results of the scenario analysis show that all regions are well on-track to eliminate leprosy, with the South and Southeast, which have the lowest incidence, likely to eliminate leprosy first. The posterior prediction plots (Fig 2) show that the fitted model estimated the observed decrease in PB incidence fairly accurately in most regions, but slightly overestimated the decrease in incidence of MB cases in all but the Midwest. It may be assumed, therefore, that these results are best-case scenarios for those regions. The predicted incidence in the Northern region is higher than has recently been predicted for Para State, which is within that region, but the time to the elimination target generally agrees between the two models [24]. All regions observed an increase in incidence up to 2003, followed by a slow decrease. This is likely due to the slow impact of control programs, rather than a change in case detection rates; chronic diseases with long latent periods, like leprosy, will require consistent control over long periods of time to reverse incidence trends.

It is important to note that the incidence of MB disease was predicted to be in the range of 13,983 to 14,913 new MB cases in Brazil in 2015. However, the North, Northeast, and Midwest are likely to require a much longer period to reach official elimination than the South and

Southeast. The best way to decrease the time to elimination would be increasing the case finding rate [45]. This would also improve the level of disability in new cases, as delay in onset of treatment is a major cause of disability. Our results, therefore, indicate that the North, Northeast, and Midwest regions of Brazil would benefit from improving the true case finding rate, which we have estimated to be slow.

Author Contributions

Conceptualization: RLS.

Data curation: RLS.

Formal analysis: RLS.

Funding acquisition: RLS.

Investigation: RLS.

Methodology:RLS.

Project administration: RLS.

Resources: RLS.

Software:RLS.

Supervision: RLS.

Validation: RLS.

Visualization: RLS.

Writing - original draft: RLS.

Writing - review & editing: RLS.

References

1. Rodrigues LC, Lockwood DNJ. Leprosy now: epidemiology, progress, challenges, and research gaps. Lancet Infect Dis. Elsevier Ltd; 2011; 11: 464–70. doi: 10.1016/S1473-3099(11)70006-8

2. Hacker MA, Sales AM, Illarramendi X, Nery JA, Duppre NC, Bastos FI, et al. A profile of patients treated at a national leprosy outpatient referral clinic in Rio de Janeiro, Brazil, 1986–2007. Rev Panam Salud Publica. 2012; 31: 485–91. Available: http://www.ncbi.nlm.nih.gov/pubmed/22858815 PMID: 22858815

3. Worobec SM. Treatment of leprosy/Hansen's disease in the early 21st century. DermatolTher. Department of Dermatology, College of Medicine, University of Illinois at Chicago, Chicago, IL 60612–7300, USA. drsophie@sbcglobal.net; 2009; 22: 518–537.

4. WHO. Eliminate Leprosy as a Public Health Problem [Internet]. 1st ed. Leprosy Elimination Group, editor. Geneva: World Health Organization; 2000. Available: http://www.who.int/lep/resources/Guide_Int_E.pdf?ua=1

5. Duarte-Cunha M, Marcelo da Cunha G, Souza-Santos R. Geographical heterogeneity in the analysis of factors associated with leprosy in an endemic area of Brazil: are we eliminating the disease? BMC Infect Dis. 2015; 15. doi: 10.1186/s12879-015-0924-x

6. Smith CS, Aerts A, Kita E, Virmond M. Time to define leprosy elimination as zero leprosy transmission? Lancet Infect Dis. Elsevier Ltd; 2016; 16: 398–399. doi: 10.1016/S1473-3099(16)00087-6

7. Lanza FM, Lana FCF. Decentralization of leprosy control actions in the micro-region of Almenara, State of Minas Gerais. Rev Lat Am Enfermagem. 2011; 19: 187–194. Available: http://www.scielo.br/scielo.php?pid=S0104-11692011000100025&script=sci_arttext PMID: 21412646

8. Dowdy DW, Golub JE, Chaisson RE, Saraceni V. Heterogeneity in tuberculosis transmission and the role of geographic hotspots in propagating epidemics. Proc Natl Acad Sci. 2012; 109: 9557–62. doi: 10.1073/pnas.1203517109 PMID: 22645356

9. Houweling TAJ, Karim-Kos HE, Kulik MC, Stolk WA, Haagsma JA, Lenk EJ, et al. Socioeconomic Inequalities in Neglected Tropical Diseases: A Systematic Review. PLoS Negl Trop Dis. 2016; 10: e0004546. doi: 10.1371/journal.pntd.0004546 PMID: 27171166

10. Fischer EAJ, de Vlas SJ, Habbema JDF, Richardus JH. The long-term effect of current and new interventions on the new case detection of leprosy: a modeling study. PLoS Negl Trop Dis. 2011; 5: e1330. doi: 10.1371/journal.pntd.0001330 PMID: 21949895

11. Meima A, Smith WCS, van Oortmarssen GJ, Richardus JH, Habbema JDF. The future incidence of leprosy : a scenario analysis. Bull World Health Organ. 2004; 82: 373–380. Available: http://www.pubmedcentral.nih.gov/articlerender.fcgi?artid=2622833&tool=pmcentrez&rendertype=abstract PMID: 15298228

12. Abubakar U. Markov decision model and the application to the cost of treatment of leprosy disease. Leonardo J Sci. 2007; 1–9. Available: http://ljs.academicdirect.org/A11/051_060.htm

13. Meima A, Gupte MD, van Oortmarssen GJ, Habbema JDF. SIMLEP: a simulation model for leprosy transmission and control. Int J Lepr other Mycobact Dis. INTERNATIONAL JOURNAL OF LEPROSY; 1999; 67: 215–236. Available: http://www-fgg.eur.nl/medbib/EUR-diss/040428_Meima_A/04.pdf

14. Abubakar U. A stochastic model in discrete states and discrete time for the control of leprosy disease. Leonardo J Sci. 2007; 1–9. Available: http://ljs.academicdirect.org/A11/051_060.htm

15. Blok D, de Vlas SJ, Fischer EAJ, Richardus JH. Mathematical Modelling of Leprosy and Its Control. Advances in Parasitology. Elsevier Ltd; 2015. pp. 33–51. doi: 10.1016/bs.apar.2014.12.002

16. Fischer EAJ, de Vlas SJ, Richardus JH, Habbema JDF. MUSIDH, multiple use of simulated demographic histories, a novel method to reduce computation time in microsimulation models of infectious diseases. Comput Methods Programs Biomed. 2008; 91: 185–90. doi: 10.1016/j.cmpb.2008.04.004 PMID: 18534713

17. Chiyaka ET. Theoretical Assessment of the Transmission Dynamics of Leprosy. Appl Math. 2013; 04: 387–401. doi: 10.4236/am.2013.42059

18. Fischer EAJ, de Vlas SJ, Meima A, Habbema JDF, Richardus JH, De Vlas SJ. Different mechanisms for heterogeneity in leprosy susceptibility can explain disease clustering within households. PLoS One. 2010; 5: S1–18. doi: 10.1371/journal.pone.0014061

19. Mushayabasa S, Bhunu CP. Modelling the effects of chemotherapy and relapse on the transmission dynamics of leprosy. Math Sci. 2012; 6: 12.

20. Meima A, Irgens LM, van Oortmarssen GJ, Richardus JH, Habbema JDF. Disappearance of leprosy from Norway: an exploration of critical factors using an epidemiological modelling approach. Int J Epidemiol. 2002; 31: 991–1009. PMID: 12435774

21. Mushayabasa S, Bhunu CP, Dhlamini M. Understanding non-compliance with WHO multidrug therapy among leprosy patients: insights from a mathematical model. In: Mushayabasa S, Bhunu C, editors. Understanding the Dynamics of Emerging and Re-Emerging Infectious Diseases using mathematical models. Kerala, India: Transworld Research Network; 2012. pp. 1–22. Available: http://www.trnres.com/ebook/uploads/steadycontent/T_1354259023Steady1.pdf

22. Smith RL, Grohn YT. Use of Approximate Bayesian Computation to assess and fit models of Mycobacterium leprae to predict outcomes of the Brazilian control program. PLoS One. 2015; 10: e0129535. doi: 10.1371/journal.pone.0129535 PMID: 26107951

23. Blok DJ, De Vlas SJ, Richardus JH. Global elimination of leprosy by 2020: are we on track? Parasit Vectors. Parasites & Vectors; 2015; 8: 548. doi: 10.1186/s13071-015-1143-4

24. de Matos HJ, Blok DJ, de Vlas SJ, Richardus JH. Leprosy New Case Detection Trends and the Future Effect of Preventive Interventions in Pará State, Brazil: A Modelling Study. PLoS Negl Trop Dis. 2016; 10: e0004507. doi: 10.1371/journal.pntd.0004507 PMID: 26938738

25. Brasil IDB. Indicadores e Dados Basicos-Brasil [Internet]. 2014. Available: http://tabnet.datasus.gov.br/cgi/idb2012/matriz.htm

26. Toni T, Welch PD, Strelkowa N, Ipsen A, Stumpf MPH. Approximate Bayesian computation scheme for parameter inference and model selection in dynamical systems. J R Soc Interface. 2009; 6: 187–202. PMID: 19205079

27. Del Moral P, Doucet A, Jasra A. An adaptive sequential Monte Carlo method for approximate Bayesian computation. Stat Comput. 2012; 22: 1009–1020. doi: 10.1007/s11222-011-9271-y

28. Brasil IDB. Indicadores e Dados Básicos—Brasil [Internet]. 2012 [cited 7 Feb 2014]. Available: http://tabnet.datasus.gov.br/cgi/idb2012/matriz.htm

29. Mushayabasa S, Bhunu CP. Modeling the impact of voluntary TESTING AND TREATMENT ON TUBERCULOSIS TRANSMISSION DYNAMICS. Int J Biomath. 2012; 5: 1–19. doi: 10.1142/S1793524511001726

30. World Health Organization. Report of the Tenth Meeting of the WHO Technical Advisory Group on Leprosy Control [Internet]. New Delhi; 2009. Available: http://www.searo.who.int/entity/global_leprosy_programme/publications/10th_tag_meeting_2009.pdf

31. Leprosy elimination: Mortality in leprosy. In: World Health Organization [Internet]. 2014 [cited 9 Mar 2014] p. 2014. Available: http://www.who.int/lep/mortality/en/

32. Bratschi MW, Steinmann P, Wickenden A, Gillis TP. Current knowledge on Mycobacterium leprae transmission: a systematic literature review. Lepr Rev. 2015; 86: 142–155. PMID: 26502685

33. The R Development Core Team. R: A Language and Environment for Statistical Computing [Internet]. R Foundation for Statistical Computing. Vienna, Austria: R; 2014. Available: http://www.r-project.org

34. Goulart IMB, Goulart LR. Leprosy: diagnostic and control challenges for a worldwide disease. ArchDermatolRes. Leprosy National Reference Center, Clinics' Hospital, School of Medicine, Federal University of Uberlandia, Uberlandia, MG, Brazil. isagoulart@centershop.com.br; 2008; 300: 269–290.

35. Rojas DE, Hernandez O, Gilt R. Some Factors Influencing Delay in Leprosy Diagnosis. Bull Pan-American Heal Organ. 1994; 28: 156–162.

36. Heijnders M. Experiencing leprosy: perceiving and coping with leprosy and its treatment. A qualitative study conducted in Nepal. Lepr Rev. 2004; 75: 327–337. Available: http://www.lepra.org.uk/platforms/lepra/files/lr/Dec04/124879.pdf PMID: 15682970

37. Henry M, GalAn N, Teasdale K, Prado R, Amar H, Rays MS, et al. Factors Contributing to the Delay in Diagnosis and Continued Transmission of Leprosy in Brazil—An Explorative, Quantitative, Questionnaire Based Study. PLoS Negl Trop Dis. 2016; 10: e0004542. doi: 10.1371/journal.pntd.0004542 PMID: 26977811

38. Lockwood DNJ, Shetty V, Penna GO. Hazards of setting targets to eliminate disease: lessons from the leprosy elimination campaign. BMJ. 2014; 348: g1136. doi: 10.1136/bmj.g1136 PMID: 24508610

39. Baena CP, Chowdhury R, Schio NA, Sabbag AE, Guarita-Souza LC, Olandoski M, et al. Ischaemic heart disease deaths in Brazil: current trends, regional disparities and future projections. Heart. 2013; 99: 1359–64. doi: 10.1136/heartjnl-2013-303617 PMID: 23886609

40. de Oliveira NPD, Barbosa IR, Paulino JN, de Camargo Cancela M, de Souza DLB. Regional and gender differences in laryngeal cancer mortality: trends and predictions until 2030 in Brazil. Oral Surg Oral Med Oral Pathol Oral Radiol. Elsevier Ltd; 2016; doi: 10.1016/j.oooo.2016.06.014

41. Bartholomay P, Pelissari DM, De Araujo WN, Yadon ZE, Heldal E. Quality of tuberculosis care at different levels of health care in Brazil in 2013. 2016; 39: 3–11.

42. Blok DJ, de Vlas SJ, Fischer EAJ, Richardus JH. Mathematical Modelling of Leprosy and Its Control. Adv Parasitol. 2015; 87: 33–51. doi: 10.1016/bs.apar.2014.12.002 PMID: 25765193

43. Lu Z, Mitchell RM, Smith RL, Van Kessel JAS, Chapagain PP, Schukken YH, et al. The importance of culling in Johne's disease control. J Theor Biol. Elsevier; 2008; 254: 135–146. doi: 10.1016/j.jtbi.2008.05.008

44. Dye C, Williams BG. The population dynamics and control of tuberculosis. Science (80-). 2010; 328: 856–61. doi: 10.1126/science.1185449

45. Kumar A, Girdhar A, Girdhar BK. Risk of developing disability in pre and post-multidrug therapy treatment among multibacillary leprosy: Agra MB Cohort study. BMJ Open. 2012; 2: e000361. doi: 10.1136/bmjopen-2011-000361 PMID: 22454186